AUTOMATIC DETECTION OF WAVE BOUNDARIES IN MULTILEAD ECG SIGNALS: VALIDATION WITH THE CSE DATABASE

by

* Pablo Laguna, Ph.D.
& Raimon Jané, Ph.D.
& Pere Caminal, Ph.D.

(*)   Departamento de Ingeniería Eléctrica Electrónica y Comunicaciones
Centro Politécnico Superior
Universidad de Zaragoza, Spain

(&)   Institut de Cibernètica.
Universitat Politècnica de Catalunya
Barcelona, Spain

Address for future correspondence:

(*)   Departamento de Ingeniería Eléctrica Electrónica y Comunicaciones
Centro Politécnico Superior
Maria de Luna, 3
50015 Zaragoza, SPAIN.

e-mail: laguna@cc.unizar.es
Telephone: 34-76-761931
          34-76-761000
FAX: 34-76-761861

ACKNOWLEDGEMENTS

Abstract

This paper presents an algorithm for automatically locating the waveform boundaries (the onsets and ends of P, QRS and T waves) in multilead ECG signals (the 12 standard leads and the orthogonal XYZ leads). Given these locations, features of clinical importance (such as the RR interval, the PQ interval, the QRS duration, the ST segment, and the QT interval) may be measured readily. First, a multilead QRS detector locates each beat, using a differentiated and low-pass filtered ECG signal as input. Next, the waveform boundaries are located in each lead. The leads in which the detected electrical activity is of longest duration are used for the final determination of the waveform boundaries. The performance of our algorithm has been evaluated using the CSE multilead measurement database. In comparison with other algorithms tested by the CSE, our algorithm achieves better agreement with manual measurements of the T wave end and of interval values, while its measurements of other waveform boundaries are within the range of the algorithm and manual measurements obtained by the CSE.

1 Introduction

The electrocardiogram (ECG) is characterized by a recurrent wave sequence (P, Q, R, S, T) associated with each beat. Various time intervals defined by the onsets and ends of these waves are important in electrocardiographic diagnosis. The most important of these intervals are the RR interval, the PQ interval, the QRS duration, the ST segment, and the QT interval. Direct measurement of these intervals requires knowledge of the locations of the boundaries (the onsets and ends) of the P, QRS and T waves.

Since beat-by-beat manual measurement of these intervals from standard 12-lead ECGs is impractical in routine clinical practice, algorithms for automated measurement have been proposed to locate QRS onsets and ends (1), QT interval limits (2), and onset of P and QRS waves and ends of P, QRS and T waves (3, 4). Although these algorithms may work acceptably given noise-free signals, their performance degrades in the presence of noise (5).

The *Common Standards for Quantitative Electrocardiography* (CSE) project, sponsored by the European Community (4), has studied the performance of many algorithms designed to locate

waveform boundaries in the ECG. An important finding of the CSE study of these algorithms is that the algorithms tend to locate the end of the T wave significantly earlier than human experts do (3). Unfortunately, no technical details are given for the algorithms used in (3, 4), limiting its use out of their domaine. All these reasons lead us to developed a new method for locating waveform boundaries, that is presented at this paper. We evaluate it using the same methods and test signals used by the CSE, and show that its agreement with manual measurements of waveform boundaries is excellent, even for measurements of the end of the T wave.

Our method is based on the multilead generalization of a previously described procedure for single-lead measurement of the QT interval (2), and subsequently used for single- and multi-lead waveform boundary determination (6, 7). The method has been applied to ECG records of the MIT-BIH database, and validated with the CSE multilead measurement database (8) where other programs have already been validated.

2   Methods

First, a multilead QRS detector (designed for 15 leads) is applied to the ECG record. Next, the algorithm estimates the waveform boundaries independently in each lead of the multilead ECG record. This procedure makes use of the differentiated ECG signal and information about wave shape. The algorithm implements criteria to establish wave presence or absence in each lead according to the relative differentiated signal magnitude in the different waves. Given the information about wave presence and the differentiated signal, the algorithm characterizes the patterns of the P wave (regular or inverted), the QRS complex (in terms of various Q, R, S, R' sequences), and the T wave (regular, inverted, or biphasic), in accordance with the classification used by the CSE working party, (9). Using the wave boundaries obtained in each lead, the final wave boundaries are selected from those leads where the detected electrical activity is longest, reducing the influence of possible noisy measurements.

Figure 1 shows the main steps of the procedure for waveform boundary detection. The multilead QRS detector includes 15 single-lead QRS detectors and generates the $QRS_j(i)$ positions of the ith

QRS in the jth lead from each lead, $\text{ECG}_j(k)$. Next, a multilead QRS decision rule gives the final $\text{QRS}_j(i)$ detections of the ith beat in each lead. We analyse each lead, $\text{ECG}_j(k)$, using the following single-lead steps: fibrillation process rejection, waveform location ($\mathbf{W}_j(i)$), and waveform boundary determination, yielding single-lead waveform boundary estimates ($\mathbf{WB}_j(i)$) for lead j and beat i. From the $\mathbf{WB}_j(i)$ estimates, a multilead waveform boundary location rule gives the final lead-independent waveform boundaries for each beat ($\mathbf{WB}(i)$). Finally, given these $\mathbf{WB}(i)$ positions, we compute the clinicaly relevant intervals (PR, QT, ...). Below, we describe these steps in greater detail.
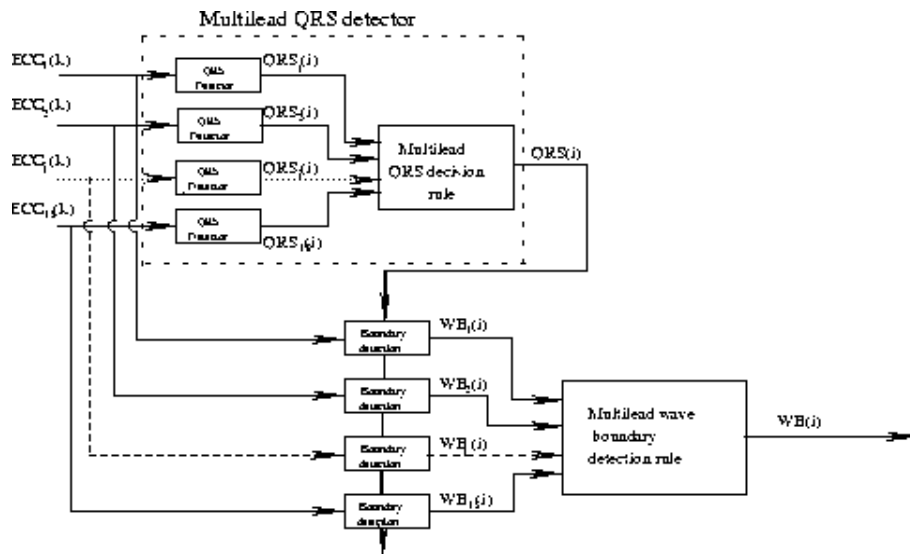

Figure 1: *Diagram of the wave boundary detection procedure*

2.1   Preprocessing:

The first step consists of a single-lead filtering process for noise reduction and a non-linear transformation to improve QRS detection (10). The linear filtering uses a second order band-pass

Lynn filter (0.8-18 Hz, -3dB) (11) to attenuate baseline drift and high frequency contamination. Once the band-pass filtered signal (ECGPB) is reached, a low-pass differentiator (10) is applied to get the information about changes in the signal slope. This differentiated signal is called ECGDER. The non-linear transformation we use is the moving-window integration of the squared signal described in (10) with an integration width of 95 ms.

2.2 QRS detection:

2.2.1 single-lead QRS detection

The single-lead QRS detector used in this work is an adaptation of that described by Pan and Tompkins (10), using the signal slope in the decision rule: any possible detection should have a maximum slope within $\pm$ 30 % of that of the previous QRS complexes.

2.2.2 Multilead QRS detection

From the estimates, $QRS_j(i)$, of the position of beat i in lead j obtained by the single-lead detectors (Fig. 1), we apply a multilead QRS detection rule to consider as QRS complexes in each lead only those whose positions do not differ more than 90 ms from one lead to the other (12). The decision rule includes the following steps:

a) The input values to this processing stage are the detected positions $QRS_j(i)$ (j=1,...,15) of the ith beat, that come from the single-lead QRS detectors. Figure 2a shows an example of these detections.

b) The first (min) and the last (max) $QRS_j(i)$ (j=1,...,15) temporal positions are searched (Fig. 2b). From these time positions we define two series of $QRS_j(i)$ positions: *series 1*, those $QRS_j(i)$ that are within 90 ms of *min*; *series 2*, those $QRS_j(i)$ that are within 90 ms of *max*. In figure 2b, *series 1* has 11 positions and *series 2* has 8 positions.
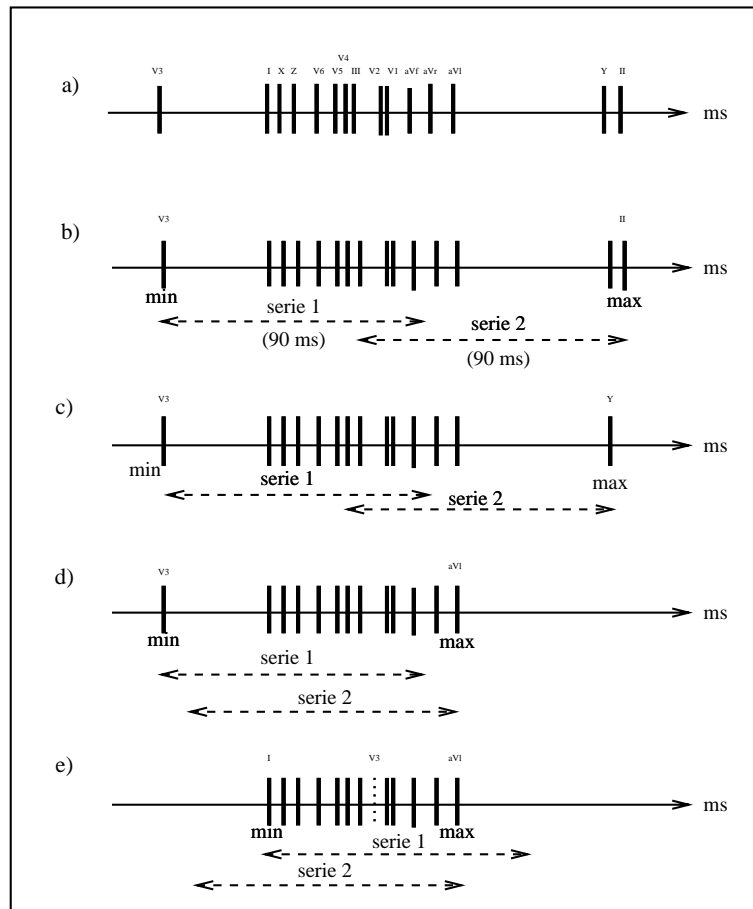
5

Figure 2: *Multilead QRS decision rule*

c) The two series are compared. If both contain all 15 QRS$_j$(i) (j=1,...,15) positions, it is assumed that the ith beat has been detected correctly in all the leads. If the series contain different numbers of positions, the extreme value (min or max) of the series that contains the smaller number of positions is rejected.

If the rejected position is max, it may result from a missed detection, and max could belong to the next beat. Thus, if max belongs to lead k, we assign QRS$_k(l)$ = QRS$_k(l-1)$ ($l \geq i+1$). In (Fig. 2b,c) the max position, belonging to lead II, is rejected as a probable false detection, and the algorithm assumes that the true QRS in lead II was missed by the single-lead detector.

If the rejected position is min, it may result from a false positive detection at this lead. In this case, if min belongs to lead k, QRS$_k$(i+1) may be the true detection for which we are looking. Thus, we may assign QRS$_k(l)$ = QRS$_k(l+1)$ ($l \geq i$). In (Fig. 2d,e) the min position, belonging to lead V$_3$, is rejected as a probable false detection, and the algorithm reassigns QRS$_{V_3}$(i+1) (dashed line) as the position of the ith beat at V$_3$.

d) The process continues recursively until both series are identical. The remaining positions are considered the true detection for the ith beat in each lead. Leads where the ith beat was not detected, or where a detection was rejected in the previous step, are not used for waveform boundary determination for beat i.

In figure 3 we have the single-lead detection marks in 7 leads of record MO1_109 from the CSE database. The multilead decision rule rejects the 12th detected beat in lead II (it was the P wave position, rather than the QRS complex position) since it is not in accordance with the other leads; and recognizes two missing beats in lead V$_3$ (7th and 11th). Table 1 summarizes the detections in this record.

2.3   Fibrillation rejection:

During fibrillation, it is meaningless to measure P, QRS and T boundaries. Fibrillation is detected using the single-lead procedure presented in (13), applied before the wave location procedure.
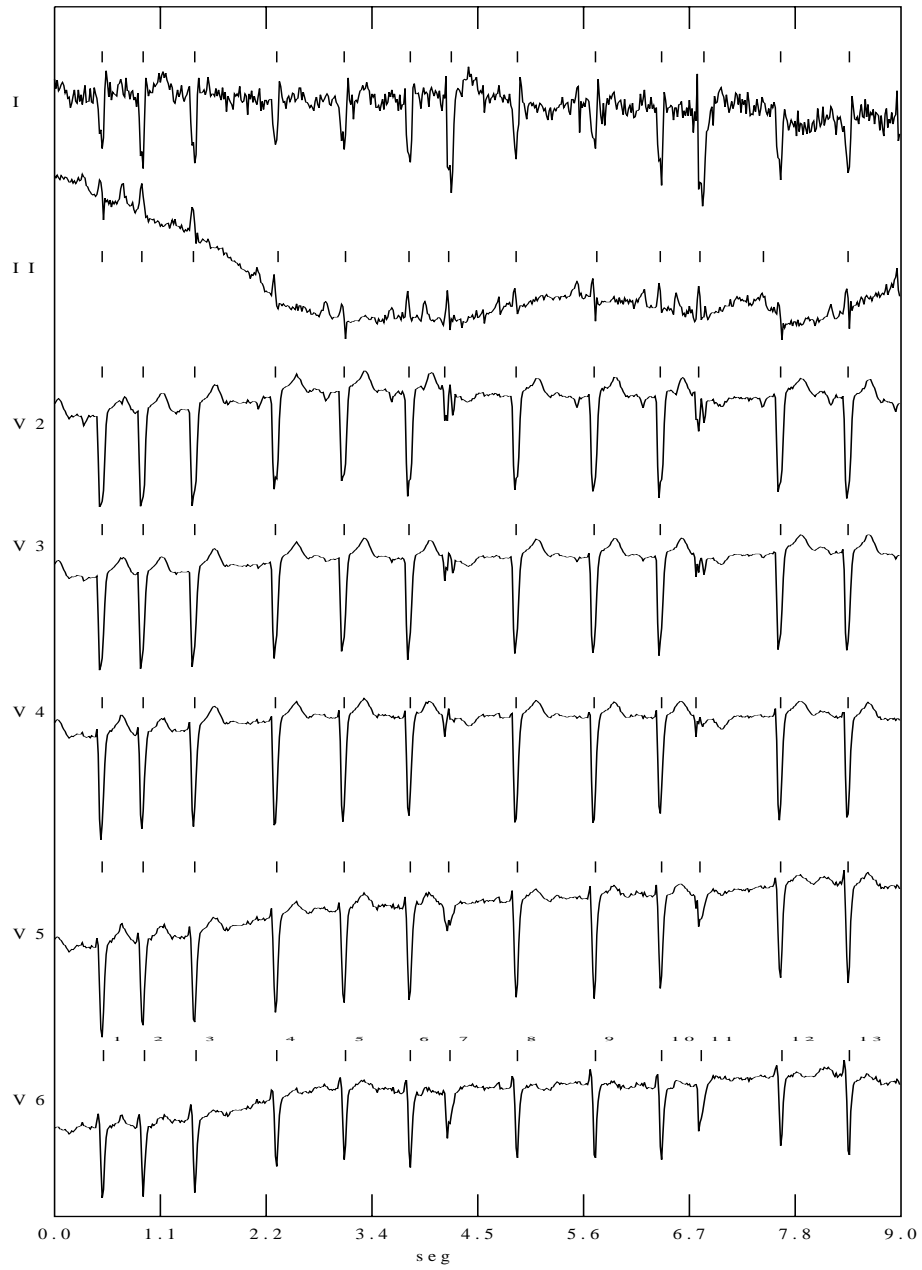
Figure 3: *Example of multilead QRS detection in record MO1_109 of the CSE database.*

8

	Leads														
Beat	I	II	III	aV$_R$	aV$_L$	aV$_F$	V$_1$	V$_2$	V$_3$	V$_4$	V$_5$	V$_6$	X	Y	Z
1	+	+	+	+	+	+	+	+	+	+	+	+	+	+	+
2	+	+	+	+	+	+	+	+	+	+	+	+	+	+	+
3	+	+	+	+	+	+	+	+	+	+	+	+	+	+	+
4	+	+	+	+	+	+	+	+	+	+	+	+	+	+	+
5	+	+	+	+	+	+	+	+	+	+	+	+	+	+	+
6	+	+	+	+	+	+	+	+	+	+	+	+	+	+	+
7	+	+	+	+	+	+	+	+	*	+	+	+	+	+	+
8	+	+	+	+	+	+	+	+	+	+	+	+	+	+	+
9	+	+	+	+	+	+	+	+	+	+	+	+	+	+	+
10	+	+	+	+	+	+	+	+	+	+	+	+	+	+	+
11	+	+	+	+	+	+	+	+	*	+	+	+	+	+	+
12	+	*	+	+	+	+	+	+	+	+	+	+	+	+	+
13	+	+	+	+	+	+	+	+	+	+	+	+	+	+	+

Table 1: *QRS detections accepted in each lead of record MO1_109 of the CSE database. The symbol (+) represents accepted detections; the symbol (*) represents beats either rejected or not detected in the corresponding lead.*

2.4   Wave location:

The QRS positions ($QRS_j(i)$) given by the detector may be Q, R or S wave peaks. The algorithm searches for the nearest peak positions before (p_b) and after (p_a) the $QRS_j(i)$ position in the ECGDER (zero-crossing in this signal). According to the polarity and relative value of these peaks, we decide if $QRS_j(i)$ belongs to the Q, the R or the S wave (2). The adjacent wave positions are detected as the nearest zero-crossing points to $QRS_j(i)$ in ECGDER. To admit these adjacent detected points as wave positions ($\mathbf{W}$(i)), the time distance between waves must be in the range of physiologically plausible intervals, and the maximum slope associated with these waves must be bigger than a threshold of the maximum slope associated with the QRS complex (*dermax*). The threshold value is experimentally adjusted and is different for Q, R, S or R' waves, ranging from 3 to 10% of the maximum QRS slope value (*dermax*). This procedure thus attempts to locate as many of the Q, R, S and R' peaks as are present.

Next, we search for the P and T wave peaks. These waves have lower frequency components than the QRS complex. We again apply a low-pass filter (-3db cutoff frequency of 12 Hz) to ECGDER to reduce remaining noise. In this filtered signal (DERFI) we define a window of 155 ms starting 225 ms before the R position. This window is shortened when the previous T or the next Q wave is in it. In this window we search for the maximum and minimum value. If these values are bigger than 2% of the maximum slope of the QRS complex, the algorithm assumes that it has located a P wave; otherwise, the algorithm assumes that the P wave cannot be located in the given lead. The P wave peak is assumed to occur at the zero-crossing between the maximum and the minimum values in the window.

To detect the T wave, we define a search window in DERFI that is a function of the heart rate (2). The algorithm determines the type of T-wave (regular, inverted, biphasic +-, or biphasic -+) according to the relative positions and values of the maximum and minimum values within the search window, using the CSE working party classification (9). The T wave peak is assumed to occur at the zero-crossing adjacent to the maximum or minimum value.

2.5 Waveform boundary location
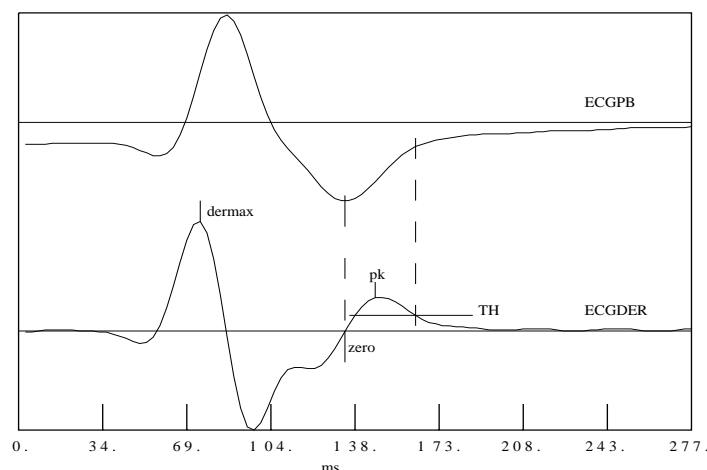
2.5.1 Single lead waveform boundary location:

Figure 4: *Determination of the end of the QRS by the threshold method.*

10

K		P wave		Q wave	R wave		S wave	T wave	
		P_b	P_e	Q_b	R_b	R_e	S_e	T_b	T_e
$\dfrac{\text{ECGDER(pk) x 10}}{dermax}$	$\leq 0{,}13$	1.35	2.0	1.8	5.0	5.0	3.0	2.0	4.0
	0,13 - 0,20								5.0
	0,20 - 0,41								6.0
	0,41 - 2,00								
	2.00 - 4.00				8.0				
	4,00 - 4,75						8.0		
	4,75 - 6,20				28		9.0		7.0
	$\geq 6{,}20$						12.0		

Table 2: *Values of the k threshold for each wave boundary: P begin (onset) P_b, P end P_e, etc, as a function of the maximum wave slope (ECGDER(k)) relative to the maximum QRS slope dermax.*

Once we have the wave locations (zero-crossing point (*zero*) in the differentiated signal ECGDER or DERFI), we proceed to locate the onset and end (boundaries) of each waveform. The differentiated threshold method used in this work was presented in (2) for QT interval determination, and in this work we have generalized it to determine any wave limit in multilead ECG records. Figure 4 shows this procedure for QRS end determination. From the *zero* point (S wave position) we search for the adjacent peak (*pk*) on the right (for the end) or on the left (for the onset). This point is the point of maximum slope in the wave. With the value of ECGDER at time instant *pk* (ECGDER(*pk*)) we define a threshold (TH) as $TH=$ECGDER(pk)/k. Thus, we determine the end (onset) point of the wave as the forward (backward) threshold crossing point from *zero* in the ECGDER signal (end of S wave in figure 4). The value of k is a constant that is experimentally adjusted and reaches its best performance with the values expresed in table 2.

When two waveforms overlap, the threshold criteria can fail and may give boundary locations far from the physiologicaly expected points. Thus, the algorithm uses a *minimum differentiated criterion* as described in figure 5. From the *pk* position we find the smallest absolute peak in the same direction (*pk'*) as for the previous criterion. This peak position, associated with an ECG

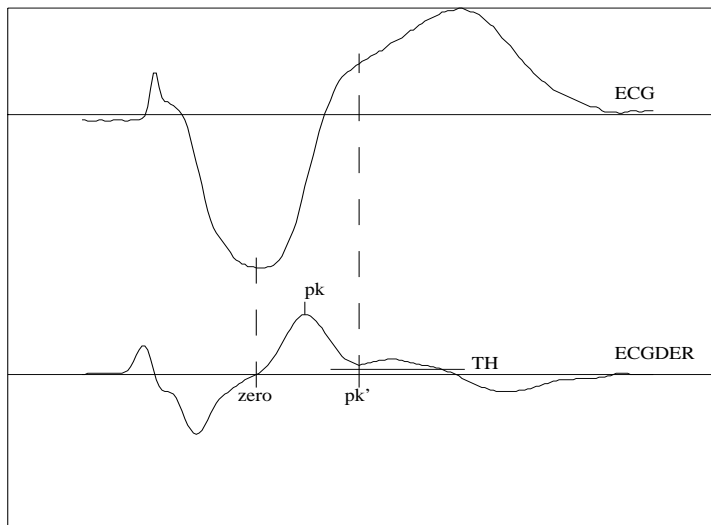inflection, is taken as the waveform boundary. (fig. 5).

Figure 5: *Minimum differentiated criterion.*

Figure 6 shows this procedure applied to a single-lead ECG record from the MIT-BIH database. The short horizontal lines at each QRS complex represent the isoelectric level calculated at each beat for wave amplitude measurement purposes. The isoelectric level is estimated as the average ECG signal between the P end (Pe) and the QRS onset (QRSb), excluding the first and last 15 ms in this interval.

In the presence of high-amplitude baseline wander, this procedure has been shown to be more robust when applied to the ECG records after removal of baseline interference, given that this interference can overlap the spectrum of the P and T waves. The use of a threshold criterion in the presence of low-frequency artifact in the differentiated signal could lead to estimation errors if no *a priori* baseline cancellation is done.

2.5.2   Multilead wave onset and end determination:

From the previous procedure we obtain, for each waveform boundary **WB**, (P_b, P_e, QRS_b, ...), a set of waveform boundary positions $\mathbf{WB}_j(i)$ belonging to beat i of lead j (j can take values from 1 to 15, except for values corresponding to the leads where no detection was made, or where the
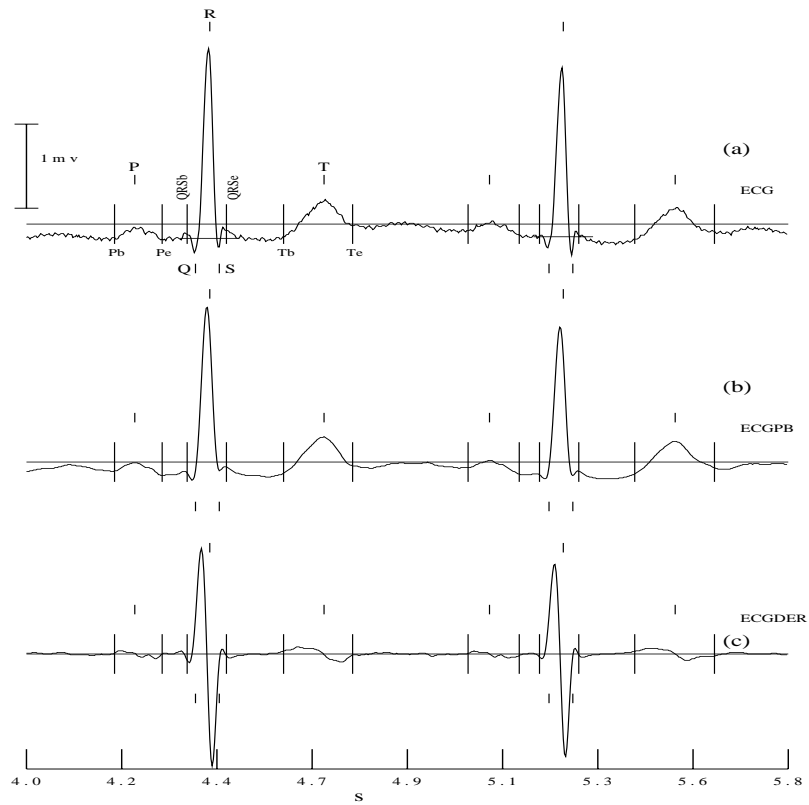
12

Figure 6: *Detection of wave boundaries in two beats belonging to record 103 (lead MLII) of the MIT-BIH ECG database. Short lines denote the wave positions (P, Q, R, S and T) and long lines the wave limits: P onset (Pb), P end (Pe), etc. a) is the original ECG, b) the ECGPB signal and c) the ECGDER signal.*

multilead QRS detection rule rejected the detection). The next step is the selection, from these $\mathbf{WB}_j$(i) positions, of the one $\mathbf{WB}$(i) that will be considered as the real onset or end of the waveform at the ith beat. Electrophysiologically, if all $\mathbf{WB}_j$(i) were correctly detected, we should select the earliest $\mathbf{WB}_j$(i) (j=1, ..., 15) for the waveform onset and the latest for the waveform end, in order to recover the boundary from that lead where the electrical activity of the heart has the longest temporal projection. However, due to noise or errors, misestimations could have occurred in the determination of some $\mathbf{WB}_j$(i), that may lead to an erroneous final $\mathbf{WB}$(i) position. To reduce the risk of this occurrence, we apply the following multilead wave boundary detection rule (figure 1) for each ith beat: We search the minimum (min) time position (for onsets) or maximum (max) time position (for ends) of $\mathbf{WB}_j$(i) (j=1, ...,15). If no more than two other leads have their $\mathbf{WB}_j$(i) mark in the interval (min, $min + \delta$) or ($max - \delta$, max), the min or max $\mathbf{WB}_j$(i) point is rejected as a possible noisy detection. The value of δ is selected according to the usual variability in manual estimations (9) and the empirical practice. Values for δ are 6, 6, 6, 10 and 12 ms for P_b, P_e, QRS_b, QRS_e, and T_e, respectively. After that we take the wave onsets (ends) as the minimum (maximum) of the remaining $\mathbf{WB}_j$(i) positions, obtaining the final $\mathbf{WB}$(i).

3   Results

The single-lead procedure has been applied to several records of the MIT-BIH database. Figure 7 shows some of the results obtained on four different records with no standar morphologies: record 106 presents a RSR' pattern, record 108 presents a QS pattern, record 114 presents a W pattern and record 111 presents a R wave with two peaks. In all cases the wave limits are well determined, including wave shape determination.

The multilead procedure has been applied to records of the CSE multilead measurements database. Figure 8 shows the multi-lead advantage of the results obtained on record MO1_063 of this database. Note how the multilead boundary location procedure improves the location of the T end point, which differs significantly between leads V_2 and V_3, and others such as I or III.
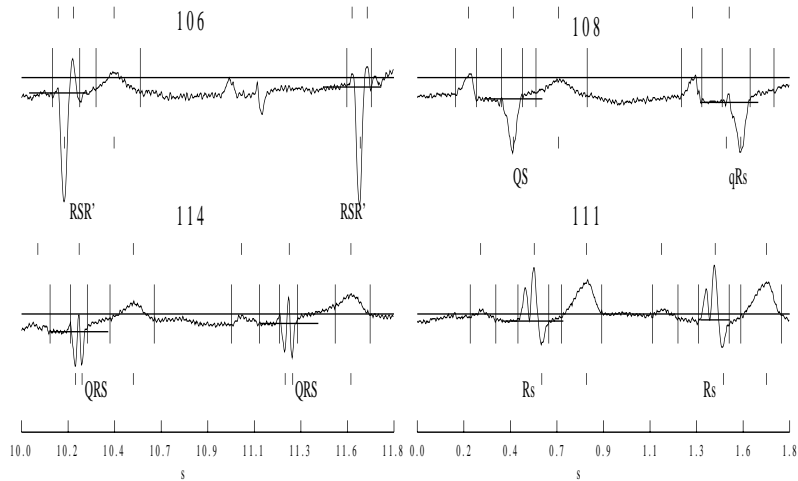
Figure 7: *Results on different ECG patterns.*

4 Validation with the CSE database

Our algorithm for locating waveform boundaries (onset and end) has been evaluated with the CSE multilead measurement database (14). The evaluation has been carried out in terms of the mean (μ) and standard deviation (σ) of the differences between the estimates obtained using our algorithm and: a) the mean referee estimates of the CSE database (RE_{CSE}), or b) the mean program estimates of the CSE database (PE_{CSE}), in each measured beat set. We have compared the performance of our algorithm against the mean performance of the algorithms tested by the CSE, because the CSE has not reported independent results from each program tested. In table 3 we present these results together with the accepted tolerance for referee deviations (σ_{ref}) reported in (9). The value n^o refers to the number of measured beats available in the CSE database for comparisons (one beat from each CSE multilead ECG records). These numbers (around 120 beats for comparison with other programs and around 30 beats for comparison with human referee measurements) are too small for to permit statistical inferences about our algorithm, but are the only accessible comparative measurements provided by the CSE database. Despite the small number of available reference measurements, we have cited these results since no other method would permit a fair comparison of our algorithm with others, or with human experts.
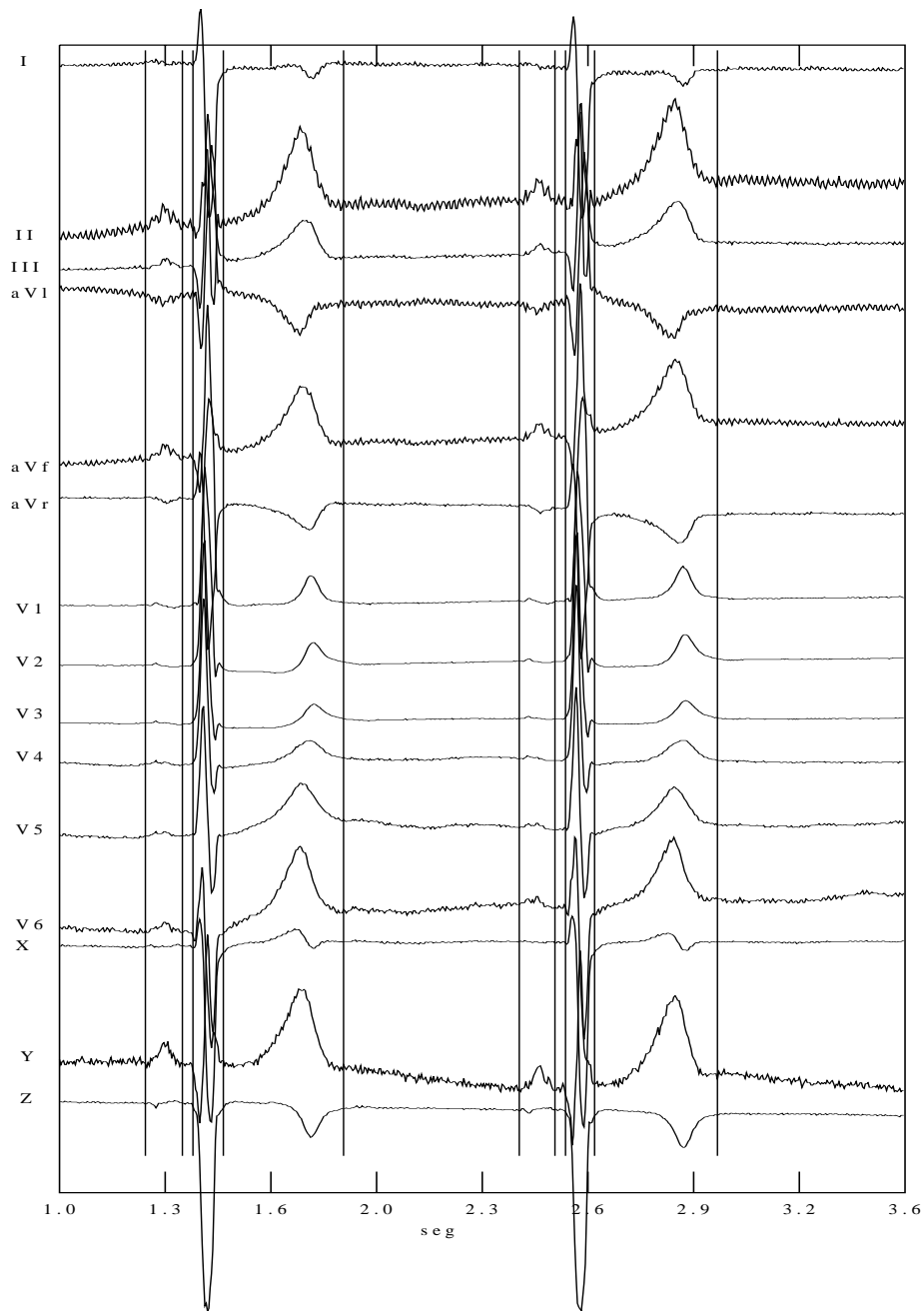
15

Figure 8: *Multilead waveform boundary determination in record MO1_063 of the CSE database.*

From table 3 we see that the our algorithm yields unbiased measurements ($\mu \leq$ sampling period = 2 ms) with standard deviations comparable to those of measurements made by human experts; hence, for the evaluation sample, our algorithm provides valid measurements. With respect to measurements of the end of the T wave, our algorithm (ME) shows much better agreement with the RE_{CSE} (1.8 ms mean difference) than for the PE_{CSE} (9.7 ms mean difference). These results suggest that our algorithm is more accurate for determination of T-wave end locations than the mean program estimates.

ME - PE_{CSE}					
	P_{on}	P_{off}	QRS_{on}	QRS_{off}	T_{off}
n^o	111	111	121	121	121
μ (ms)	-0.072	0.505	-3.587	0.083	9.700
σ (ms)	5.695	8.310	4.193	7.705	16.467
ME - RE_{CSE}					
	P_{on}	P_{off}	QRS_{on}	QRS_{off}	T_{off}
n^o	30	29	30	25	26
μ (ms)	1.000	-1.034	-2.067	-0.160	1.846
σ (ms)	7.926	5.144	7.437	7.893	10.552
Accepted tolerances for referee deviations (9)					
σ_{ref}	10.2	12.7	6.5	11.6	30.6

Table 3: *Evaluation results, comparing the waveform boundary detection method estimates (ME) with the mean referee estimates (RE_{CSE}) and with the mean program estimates (PE_{CSE}).*

We have also evaluated our algorithm in terms of the significant interval values: P duration (P-DUR), PR interval (PR-INT), QRS duration (QRS-DUR) and QT interval (QT-INT). The evaluation has been done in terms of the mean and standard deviation of the differences between intervals estimated by our algorithm (ME) and: *a)* the intervals measured from the mean referee estimates of CSE database (RE_{CSE}), or *b)* the intervals measured from the mean program estimates

of CSE database (PE_{CSE}). In table 4 we present these results together with the interval measure tolerances, mean (μ_{tol}) and standard deviation (σ_{tol}) reported in (15). The value n^o refers to the number of measured beats available in the CSE database for comparisons.

ME - PE_{CSE}				
	P-DUR	QRS-DUR	PR-INT	QT-INT
n^o	111	121	111	121
μ(ms)	0.577	3.802	-3.423	13.133
σ(ms)	10.690	9.050	6.803	16.831
ME - RE_{CSE}				
	P-DUR	QRS-DUR	PR-INT	QT-INT
n^o	25	23	25	23
μ(ms)	-0.400	3.217	-2.400	4.261
σ(ms)	7.095	9.812	8.679	10.274
Error limit tolerances for programs (15)				
μ_{tol}(ms)	10.0	3.5	4.5	7.0
σ_{tol}(ms)	12.0	8.0	8.0	13.5

Table 4: *Evaluation results, comparing the ECG interval values measured from the waveform boundary method estimates (ME) with those measures from the mean referee estimates (RE_{CSE}) and with the mean program estimates (PE_{CSE}).*

From this table we see that the interval measures obtained with the proposed method have mean differences and standard deviations within the expert tolerance limits.

5 Conclusions

Our algorithm for locating waveform boundaries in the ECG has been shown to be robust when noise is present. The multilead QRS detector retains the single-lead QRS information, rejecting

those detections that can be identified as erroneous when compared with other leads, which are not possible to reject using only one lead. The availability of single-lead QRS detection marks permits the use of a single-lead procedure for boundary detection; this procedure in turn permits recovery of the temporal projections of cardiac electrical activity. The final decision is taken on the basis that the larger temporal duration of a wave in one lead should not differ significantly from at least a subset of the other leads, allowing the algorithm to reject erroneous measurements due to noise, and to detect the larger temporal projection of the wave that is the final objective of the method.

The difficulty of establishing an analytical rule that unambigously locates the wave boundaries is solved in this work through a threshold that is adjusted by a constant (k) to be in the highest possible agreement with manual expert measurement. Using additional training data might lead to minor adjustments in the value of k, but we would not expect significant changes (since the ECG records of the CSE database already contain a large variety of ECG morphologies). We have shown that the measurements of clinically important intervals obtained using our algorithm are comparable in accuracy with those obtained by human experts. In particular, our algorithm agrees better with human expert measurements of the end of the T wave than did the algorithms studied by the CSE. It is important to note, however, that these findings were obtained using only the limited number of ECG records included in the CSE database.

The information about waveform shape obtained with this method is very useful for ECG classification and cardiac diagnosis. The detection of the T wave onset allows further measures of the ST segment (12). The interval values, wave amplitudes, patterns of P, QRS and T waves, and wave presence or absence, could be used to help cardiac diagnosis presenting statistical and trend displays to the medical expert. Also this information can be the input to a system that allows automatic cardiac diagnosis from ECG analysis. The algorithm at present works on either on a VMS station or a UNIX machine taken as inputs the digitized ECG records.

19

6   References

1. **Nygärds M.E.**, and Sörnmo L. (1983.) "Delineation of the QRS complex using the envelope of the e.c.g.", *Med. & Biol. Eng. & Comput.* **21**, 538-547.

2. **Laguna P.,** Thakor N.V., Caminal P., Jané R., and Hyung-Ro Y. (1990) "New algorithm for QT interval analysis in 24 hour Holter ECG: Performance and applications". *Med. & Biol. Eng. & Comput.* **28**, 67-73. 1990.

3. **Willems J.L.** *et al.* (1985) "Assessment of the performance of electrocardiographic computer programs with the use of a reference database", *Circulation*, **71**, 523-534.

4. **Willems J.L.** *et al* (1990) "Common Standards for Quantitative Electrocardiography: Goals and main results" *Meth. Inform. Med.* **29**, 263-271.

5. **Willems J.L.**, Zywietz C., Arnaud P., Van Bemmel J.H., Degani R., and Macfarlane W. (1987a) "Influence of noise on wave boundary recognition by ECG measurement programs", *Computers and Biomedical Research,* **20**, 543-562.

6. **Laguna P.,** Bogatell E., Jané R., and Caminal P. (1991) "Automatic detection of characteristic points in the ECG" *Proc. of the IV Int. Symposium on Biomedical Engineering.*, Peñiscola, Spain. 338-339.

7. **Laguna P.,** Vigo D., Jané R., and Caminal P. (1992) "Automatic wave onset and offset determination in ECG signals: Validation with the CSE database" *In Computers in Cardiology*, IEEE Society Press, 167-170.

8. **Willems J.L.**, Arnaud P., Van Bemmel J.H., Bourdillon P.J., Degani R., Denis B., Graham I., Harms F.M.A., Macfarlane W., Mazzocca G., Meyer J., and Zywietz C. (1987b) "A reference data base for multilead electrocardiographic computer measurement programs", *Journal of American College of Cardiology,* **10**, n° 6. 1313-1321.

9. **The CSE working party** (1985) "Recomendations for measurement standards in quantitative electrocardiography", *European Heart Journal*, **6**, 815-825.

10. **Pan J.,** and Tompkins W.J. (1985) "A real-time QRS detection algorithm", *IEEE Trans. Biomed. Eng.,* **BME-32**, n. 3, 230-236.

11. **Lynn P.A.,** (1977) "Online digital filters for biological signals: some fast designs for a small computer", *Med. & Biol. Eng. & Comput.,,* **15** 534-540.

12. **Webster J.G.,** (1988) "Enciclopedia of medical devices and instrumentation", *John Wiley & ons, New York.*

13. **Thakor N.V.,** Zhu Y., and Pan K. (1990) "Ventricular Tachycardia and Fibrillation Detection by a Sequential Hypothesis Testing Algorithm", *IEEE Trans. Biomed. Eng.,* **37**, n. 9, 837-843.

14. **Willems J.L.** (1988) "Common standards for quantitative electrocardiography. CSE multilead atlas", *Leuven,* ACCO Publ. 1-341.

15. **Zywietz C.,** and Celikag D. (1992) "Testing results and derivation of minimum performance criteria for computerized ECG-analysis", *Computers in Cardiology,* IEEE Computer Society Press, Venecia, 97-100.

ACKNOWLEDGEMENTS